Available online at www.sciencedirect.com
ScienceDirect
Journal of Sound and Vibration 324 (2009) 1141–1157
JOURNAL OF SOUND AND VIBRATION
www.elsevier.com/locate/jsvi

Robust health evaluation of gearbox subject to tooth failure with wavelet decomposition

Dong Wang[a], Qiang Miao[a,*], Rui Kang[b]

[a]School of Mechatronics Engineering, University of Electronic Science and Technology of China, Chengdu, Sichuan 610054, PR China
[b]Department of System Engineering of Engineering Technology, BeiHang University, Xueyuan Road No.37, Haidian District, Beijing 100083, PR China

Received 25 June 2008; received in revised form 10 November 2008; accepted 12 February 2009
Handling Editor: L.G. Tham
Available online 17 March 2009

Abstract

Machinery condition monitoring is a key step to perform condition-based maintenance (CBM) policy. In this paper, a novel health evaluation method based on wavelet decomposition is proposed. In the process of wavelet decomposition, a new index is defined to choose the optimal detail signal. After that, frequency spectrum growth index (FSGI) is proposed to serve as a quantitative description of machine health condition. This index is helpful for maintenance decision-making. At the same time, a semi-dynamic threshold criterion that can be used to check the existence of fault is established. In order to demonstrate the performance of this index with its semi-dynamic threshold, a comprehensive study with three sets of vibration data collected from a mechanical diagnostics test bed is conducted to validate this method. The analysis results indicate that the proposed method is insensitive to the selection of wavelet function and wavelet decomposition level, which means that FSGI has excellent performance in gear early fault detection.

1. Introduction

Due to over-maintenance or under-maintenance problems in traditional maintenance strategies, research on condition-based maintenance (CBM) becomes more popular than before in recent years. In CBM implementation, condition monitoring is a key step which provides critical information for maintenance decision-making. To detect condition of machinery, much information can be utilized, such as vibration, acoustic emission, temperature, etc. It is appropriate for us to use vibration-based method because vibration measurements usually include abundant information of machinery and overhead of vibration-based method is relatively low. Until now, a lot of research has been done in this area and a review on this topic can be found in Ref. [1].

To identify incipient condition changes in the process of condition monitoring, a health index is usually necessary, which is a quantitative description of machinery health condition. Compared with other fault diagnosis schemes, health index provides an intuitive way to describe machinery health condition and it can be

*Corresponding author.
E-mail addresses: wangdonguestc@yahoo.cn (D. Wang), mqiang@uestc.edu.cn (Q. Miao), kangrui@buaa.edu.cn (R. Kang).

0022-460X/$ - see front matter © 2009 Elsevier Ltd. All rights reserved.
doi:10.1016/j.jsv.2009.02.013

used for maintenance decision modeling [2]. However, due to weak fault characteristics at the beginning of machine failure, it is difficult to tell when incipient fault occurs.

The research in this paper is to investigate a method for machinery health evaluation using health index. Currently, wavelet analysis has been accepted as a powerful tool that decomposes a signal into different scales corresponding to different frequency bandwidths [3]. Ref. [4] gives a summary of recent applications on wavelet analysis. Regarding current progresses in machinery health evaluation, Miao et al. [5] applied singularity analysis with wavelet to gain Lipchitz exponent function and a kurtosis based health index was proposed. Lin et al. [2] used residual error signal for construction of gearbox health index, together with the proportional-hazard modeling technique for CBM analysis. The two aforementioned indexes are validated by the data obtained from gearboxes on a mechanical diagnostic test-bed (MDTB), which are provided by Applied Research Laboratory (ARL) at Pennsylvania State University.

Along with this work, this paper proposes a novel health index called frequency spectrum growth index (FSGI) to detect health condition of gear, which is on the basis of wavelet decomposition. At the same time, a semi-dynamic threshold criterion that can be used to check the existence of failure is established. To validate the performance of proposed index, three sets of vibration data obtained from MDTB are utilized in this research. Compared with other research on the application of wavelet, the proposed health index is insensitive to the selection of wavelet function and wavelet decomposition level. Thus, it has better potential in industry application.

The rest of this paper is organized as follows. Section 2 briefly introduces wavelet transform. In Section 3, a novel condition monitoring index for gear is proposed, together with optimal detail signal selection and a semi-dynamic threshold criterion. In Section 4, the data from TR#5 are firstly used to illustrate how to choose the optimal detail signal after wavelet decomposition. To evaluate the impact of wavelet function and wavelet decomposition level on proposed health index, several comparison studies are conducted with different wavelet functions and decomposition levels. After that, the proposed method with same wavelet function at different orders is analyzed to observe the effect on index. In order to comprehensively investigate the capability of this index, a comparison with another index is conducted using more data from TR#10 and TR#12. Conclusions are summarized in the end.

2. Signal decomposition with wavelet

Continuous wavelet transform (CWT) of a finite-energy signal can be defined as the integral of a signal $x(t)$ multiplied by scaled and shifted versions of a basic wavelet function $\psi(t)$ [6], i.e.

$$W(a,b) = \int_R x(t)\frac{1}{\sqrt{a}}\psi^*\left(\frac{t-b}{a}\right)\mathrm{d}t, \quad a \in R^+, \ b \in R, \tag{1}$$

where R^+ and R represent positive real number and real number, respectively. a and b are scaling parameter and translation parameter, respectively. * means conjugate operation. Wavelet function $\psi(t)$ should satisfy the following admissibility criterion:

$$C_\psi = \int_R \mathrm{d}\omega|\hat{\psi}(\omega)|^2|\omega|^{-1} < \infty, \tag{2}$$

where $\hat{\psi}(\omega)$ denotes Fourier transform of $\psi(t)$.

According to Eq. (1), we know that $W(a,b)$ is defined on an a–b plane, where scaling parameter a and translation parameter b are used to adjust frequency and time location of wavelet $\psi(t)$ by

$$\psi_{(a,b)}(t) = \frac{1}{\sqrt{a}}\psi\left(\frac{t-b}{a}\right), \quad a \in R^+, \ b \in R. \tag{3}$$

Here, $\sqrt{a}$ is used for energy preservation. Small scaling parameter a corresponds to high-frequency component. Translation parameter b represents the location of wavelet function in time domain. According to Eq. (1), wavelet coefficient $W(a,b)$ is able to measure similarity between signal $x(t)$ and wavelet $\psi(t)$ at different frequencies determined by scaling parameter a and different time locations determined by translation parameter b.

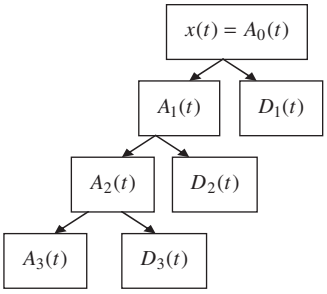

Fig. 1. An example of a three-level wavelet decomposition tree.

Discrete wavelet transform (DWT) is derived from CWT, where scales and positions are commonly chosen based on a power of 2, i.e. dyadic scales and positions [7], through

$$a = 2^j, \quad b = k2^j, \quad j,k = \{0, \pm 1, \pm 2, \ldots\}. \tag{4}$$

Discrete wavelet function and scaling function are defined as

$$\psi_{j,k}(t) = 2^{-j/2}\psi(2^{-j}t - k), \tag{5}$$

$$\phi_{j,k}(t) = 2^{j/2}\phi(2^{-j}t - k). \tag{6}$$

DWT can be implemented by filter operation. The filters used in DWT contain high-pass filter (wavelet filter) and low-pass filter (scaling filter) that are constructed, respectively:

$$g(n) = \frac{1}{\sqrt{2}}\langle \psi(t), \psi(2t - n)\rangle = (-1)^n h(1 - n), \tag{7}$$

$$h(n) = \frac{1}{\sqrt{2}}\langle \phi(t), \phi(2t - n)\rangle. \tag{8}$$

A fast wavelet transform proposed by Mallat [7] is able to perform two opposite operations, i.e. decomposition and reconstruction. In decomposition operation, a discrete signal is convolved with a low pass filter and a high pass filter, respectively. Let $x(t) = A_0(t)$, the decomposition process can be repeated as follows:

$$A_{j-1}(t) = A_j(t) + D_j(t), \tag{9}$$

where $A_j(t)$ and $D_j(t)$ are called approximation and detail signals at the jth decomposition level, respectively. In reconstruction, a pair of low-pass and high-pass reconstruction filters are convolved with $A(t)$ and $D(t)$, respectively.

In the process of wavelet decomposition, we need to firstly determine the decomposition level J. In case the decomposition level is J, then we can obtain detail signals $D_j(t)$ with $j = 1, 2, \ldots, J$. Fig. 1 shows wavelet tree of wavelet decomposition at level 3. $A_j(t)$ includes $N/2^j$ coefficients, where N is the length of original signal $x(t)$. Information obtained by DWT on each scale corresponds to a frequency bandwidth $F_s/2^{j+1}$, where F_s is sampling rate. The original signal can then be reconstructed by the sum of $A_j(t)$ and $D_j(t)$ by Eq. (9). It is also easy to obtain a reconstructed signal in a desired frequency bandwidth by setting wavelet transform coefficients beyond the desired frequency bandwidth to zero. This paper decomposes signal into different parts along this way.

3. A novel method for condition monitoring

Condition monitoring performed in this research can be illustrated in Fig. 2. Generally, it consists of four steps. Firstly, data are collected. Secondly, data are decomposed into different detail signals using wavelet analysis and an optimal detail signal is selected with the largest spectrum amplitude index (SAI), which will be

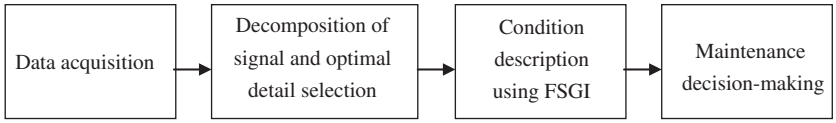

Fig. 2. Flow chart of CBM program in this paper.

introduced in Section 3.2. Thirdly, a health index FSGI proposed in this paper is calculated to describe health condition of system using the aforementioned optimal signal. At last, maintenance decision-making can be conducted. The work included in this paper mainly focus on the second and third steps.

3.1. Analysis of gear vibration signals

Suppose a pair of normal gears mesh under a constant load and speed, construction of simulated gear vibration signal is based on theoretical gear meshing vibration function [8], and is represented by

$$x(t) = \sum_{m=0}^{M} X_m \cos(2\pi m N f_s t + \phi_m), \tag{10}$$

where M is the number of tooth-meshing harmonics, N is the number of gear teeth, X_m and ϕ_m are the amplitude and the initial phase of the mth meshing harmonic ($m \times N \times f_s$), respectively. Here, meshing frequency is Nf_s. Eq. (10) tells us that the meshing frequency and its harmonics of the vibration signal obtained from a normal gearbox account for predominant frequency components.

When a fault occurs on gear tooth, sidebands appear around each meshing frequency and harmonics on both sides because of amplitude modulation (AM) and phase modulation (PM). Modulated gear vibration signal is herein described by

$$x(t) = \sum_{m=0}^{M} X_m(1 + a_m(t)) \cos(2\pi m N f_s t + \phi_m + b_m(t)), \tag{11}$$

where $a_m(t)$ and $b_m(t)$ are called amplitude and phase-modulating functions, respectively. They are given as follows:

$$a_m(t) = \sum_{n=0}^{M_1} A_{mn} \cos(2\pi f_s t + \alpha_{mn}), \tag{12}$$

$$b_m(t) = \sum_{n=0}^{M_1} B_{mn} \cos(2\pi f_s t + \beta_{mn}), \tag{13}$$

where M_1 is the number of sidebands around tooth-meshing harmonics. A_{mn} and B_{mn} are, respectively, amplitudes of the nth sideband at the mth meshing harmonic for AM and PM signals. α_{mn} and β_{mn} are phases of the nth sideband at the mth meshing harmonic for AM and PM signals, respectively. It is notable that the frequency components $mNf_s \pm nf_s$ appear in frequency spectrum due to AM and PM. Therefore, it is very important for us to detect these sidebands in fault diagnosis and condition monitoring.

3.2. Vibration signal processing

According to the flow chart described in Fig. 2, decomposition of a vibration signal is the first step after data acquisition. Wavelet transformation in general is better suitable to analyze non-stationary signals. After we decompose a signal into some parts, then we can obtain frequency spectrum of each part, respectively. Under normal condition, amplitude of a normal characteristic frequency (e.g., meshing frequency of gearbox) and its harmonics are dominant, together with randomly and evenly distributed frequency components caused by noise. However, in case of failure, fault related characteristic frequencies will be modulated and the

distribution of frequency spectrum changes [9]. Though many wavelet functions have been developed until now, Morlet wavelet [10] and Daubechies [7,9–11] wavelet were mostly used to extract fault signatures. For example, the work of Prabhakar et al. [11] and Fan and Zuo [12] indicated the feasibility of Daubechies wavelets in their research. Prabhakar et al. used DWT to detect ball bearing race faults at the fourth level. Fan and Zuo used Hilbert and wavelet packet transform to detect gearbox fault at the fourth decomposition level. However, selection of wavelet is still a problem that may have significant impact on performance of condition monitoring. In this paper, DWT with different wavelets are investigated for signal analysis and health index is established using DWT at an optimal decomposition level.

As we know, detail signals obtained in the process of wavelet decomposition correspond to different frequency bands [9]. Since the existence of failure usually produces vibration signatures at certain frequencies, it is necessary to select optimal detail signals for further fault detection. In case a gear has a local fault, AM and PM exist, which are periodic with the rotation frequency of gear. Thus, the most important components in vibration signal of fault gear are tooth-meshing frequency and its harmonics, together with sidebands. Suppose that sampling frequency is F_s, the number of gear teeth is N, rotating speed of gear is f_s, and $D_j(t)$, $j = 1, 2, \ldots, J$ is detail signal at order j. Therefore, when signal is decomposed into J details, $[F_s/2^{j+1}, F_s/2^j]$ represents the frequency range of $D_j(t)$. The frequency range of an optimal detail signal should contain $mNf_s \pm nf_s$ caused by gear fault because such kind of energy increase on sidebands often indicates fault condition. Integer m means the harmonic order of Nf_s and is selected 1 for simplification. However, it is possible that these characteristic frequencies may be close to the frequency range boundary of a detail, and it is hard to choose which detail is better since the two adjacent and orthogonal details may cover the parts of $Nf_s \pm nf_s$ bandwidth. In order to deal with this problem, perform spectrum analysis of $D_j(t)$ by

$$ES_j(f) = \left| \int_{-\infty}^{+\infty} D_j(t)\, \mathrm{e}^{-2\mathrm{i}ft\pi}\, \mathrm{d}t \right|, \quad j = 1, 2, \ldots, J. \tag{14}$$

Here, $ES_j(f)$ denotes absolute value of Fourier transform amplitude of the jth detail signal $D_j(t)$.

Compared with a normal gear, summation of these amplitude values of spectrum will increase greatly for a faulty gear. Therefore, for each $ES_j(f)$, it is reasonable to adopt both $\max\{ES_j(kf^*)|k = 1, 2, \ldots, 5\}$ and $\sum_{f=f^*,2f^*,\ldots,5f^*} ES_j(f)$ to reflect the maximum fault frequency and its harmonic components in the frequency domain and the summation of spectral amplitudes, respectively. Usually, f^* represents fault characteristic frequency. Integer k means harmonic order of f^* and k is selected from 1 to 5. This provides a way to select optimal D_j, which contains the most valuable information generated by gear fault. Therefore, SAI is defined by

$$\mathrm{SAI}_j = \log_{10}\{\max\{ES_j(kf^*)|k = 1, 2, \ldots, 5\} \times \sum_{f=f^*,2f^*,\ldots,5f^*,} ES_j(f)\}, \quad j = 1, 2, \ldots, J. \tag{15}$$

In typical applications, machine speed may have some fluctuations and f^* may not exactly match theoretical value calculated based on rotating speed of shaft. Thus, we choose both $f^* \pm 2$ Hz and $k \times (f^* \pm 2)$ in this research to compute SAI_j. D_j with the largest SAI_j can be treated as the optimal detail signal for fault signature extraction. Through this process, a time domain vibration signal D_j is transformed into frequency domain. In the following sections, we will use the jth detail signal D_j for gear condition monitoring.

3.3. Proposed health index based on optimal detail signal

While gear with fault is operating, energy of fault vibration signal changes with frequency distribution. As stated in Section 3.2, $ES_j(f)$ is the spectrum of the jth order detail signal $D_j(t)$ with the largest SAI_j and it can reflect this change better compared with all other detail signals obtained by wavelet decomposition. Based on above analysis, a novel FSGI is proposed by calculating the summation of $ES_j(f)$, i.e.

$$\mathrm{FSGI}(t) = \log_{10} \sum_f (ES_j(f)), \quad t = 1, 2, \ldots, n. \tag{16}$$

Here, subscript j means the optimal spectrum level and variable t corresponds to machinery running time. Since we will use whole lifetime gearbox vibration data to validate the proposed FSGI and vibration data are

collected and numbered consequently along with the running of test, time t is consistent with file number and is represented by file number (1,2,…,n,…).

In order to detect the occurrence of gear fault, a semi-dynamic threshold Th(t) is defined as below:

$$\mathrm{Th}(t)=\begin{cases}\dfrac{\sum_{b=1}^{t}\mathrm{FSGI}(b)}{t}+3\times\left(\dfrac{\sum_{b=1}^{t}\left(\mathrm{FSGI}(b)-\dfrac{\sum_{b=1}^{t}\mathrm{FSGI}(b)}{t}\right)^2}{t}\right)^{1/2}, & t=1,2,\ldots,t_{\mathrm{early}},\\ \dfrac{\sum_{b=1}^{t_{\mathrm{early}}}\mathrm{FSGI}(b)}{t_{\mathrm{early}}}+3\times\left(\dfrac{\sum_{b=1}^{t_{\mathrm{early}}}\left(\mathrm{FSGI}(b)-\dfrac{\sum_{b=1}^{t_{\mathrm{early}}}\mathrm{FSGI}(b)}{t_{\mathrm{early}}}\right)^2}{t_{\mathrm{early}}}\right)^{1/2}, & t=t_{\mathrm{early}}+1,t_{\mathrm{early}}+2,\ldots,n.\end{cases}\tag{17}$$

Here, semi-dynamic means the proposed threshold is not a fixed value and changes with the history value of FSGI before the occurrence of early failure. In case the current FSGI is higher the corresponding threshold for the first time (t_{early}), we conclude that the incipient fault occurs. Then, the semi-dynamic threshold becomes a fixed value.

4. Experimental validation

4.1. Test rig description

In this paper, three sets of vibration signals collected from a mechanical diagnostics test bed (MDTB) (shown in Fig. 3) are used to validate the proposed health index FSGI. These vibration data are provided by ARL at Pennsylvania State University on three test runs of single reduction helical gearboxes [13], which are named as TR#5, TR#10 and TR#12, respectively. For each test run, data were collected until the MDTB was shutdown. So, there were a series of inspections performed in the process of test run. Each inspection generated a piece of signal collected in a 10 s window at sampling rate of 20 kHz. The signal was saved as a

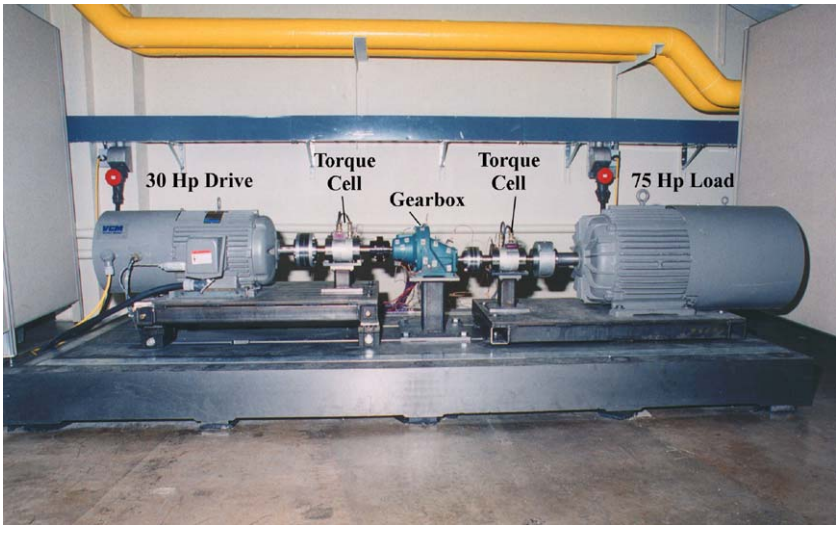

Fig. 3. Mechanical diagnostic test bed.

data file and numbered consequently. For example, the relationship between the file number and timestamp for TR#5 is presented in Table 1.

The test rig was in a brand-new state at the beginning of each experiment and ran until gear tooth failure. In addition, each experiment included two kinds of workload conditions, i.e. it started at normal workload (Condition #1) and the workload was doubled or tripled (Condition #2) after some time to accelerate the experiment. Tables 2–4 provide the test run time specifications of TR#5, TR#10 and TR#12. The mechanical

Table 1
The relationship between timestamp and file number for TR#5.

Timestamp	Date time	t
0	6/19 14:00:03	1
16	6/19 22:00:03	2
32	6/20 06:00:01	3
48	6/20 14:00:02	4
64	6/20 22:00:02	5
80	6/21 06:00:03	6
96	6/21 14:00:02	7
112	6/21 22:00:03	8
128	6/22 06:00:03	9
144	6/22 14:00:02	10
160	6/22 22:00:02	11
176	6/23 06:00:01	12
192	6/23 14:00:02	13
193	6/23 14:30:03	14
194	6/23 15:00:02	15
195	6/23 15:30:03	16
196	6/23 16:00:02	17
197	6/23 16:30:02	18
198	6/23 17:00:03	19
199	6/23 17:30:03	20
200	6/23 18:00:02	21
201	6/23 18:30:07	22
202	6/23 19:00:02	23
203	6/23 19:30:02	24
204	6/23 20:00:02	25
205	6/23 20:30:06	26
206	6/23 21:00:02	27
207	6/23 21:30:02	28
208	6/23 22:00:02	29
209	6/23 22:30:03	30
210	6/23 22:34:05	31
211	6/23 23:00:02	32
212	6/23 23:18:49	33
213	6/23 23:30:03	34
214	6/24 00:00:03	35
215	6/24 00:30:03	36
216	6/24 00:54:20	37
217	6/24 01:00:03	38
218	6/24 01:30:02	39
219	6/24 02:00:03	40
220	6/24 02:30:03	41
221	6/24 03:00:03	42
222	6/24 03:30:04	43
223	6/24 04:00:03	44
224	6/24 04:30:02	45
225	6/24 05:00:02	46
226	6/24 05:07:09	47

Table 1 (*continued*)

Timestamp	Date time	t
227	6/24 05:30:02	48
228	6/24 06:00:02	49
229	6/24 06:30:02	50
230	6/24 06:35:32	51
231	6/24 07:00:02	52
232	6/24 07:30:03	53
233	6/24 08:00:02	54
234	6/24 08:30:03	55
235	6/24 09:00:03	56
236	6/24 09:30:02	57
237	6/24 10:00:03	58
238	6/24 10:30:02	59
239	6/24 11:00:03	60
240	6/24 11:30:02	61
241	6/24 11:47:00	62
242	6/24 12:00:02	63
243	6/24 12:30:02	64
244	6/24 13:00:03	65
245	6/24 13:30:03	66
246	6/24 14:00:02	67
247	6/24 14:30:02	68
248	6/24 15:00:02	69
249	6/24 15:30:02	70
250	6/24 16:00:03	71
251	6/24 16:07:06	72
252	6/24 16:15:42	73
253	6/24 16:30:02	74
254	6/24 17:00:02	75
255	6/24 17:30:02	76
256	6/24 18:00:04	77
257	6/24 18:30:14	78
258	6/24 19:00:02	79
259	6/24 19:30:06	80
260	6/24 20:00:05	81
261	6/24 20:30:02	82
262	6/24 20:56:35	83

Table 2
Time specification of workload change in TR#5.

	Time period	Time stamp	File number	Workload
Condition #1	6/19/97 13:35 (GMT)–6/23/97 13:35 (GMT)	000–176	1–12 (100% max)	540 in-lbs
Condition #2	6/23/97 13:35 (GMT)–6/24/97 20:56 (GMT)	192–262	13–83 (300% max)	1620 in-lbs

Table 3
Time specification of workload change in TR#10.

	Time period	Time stamp	File number	Workload
Condition #1	11/17/97 16:20 (GMT)–11/21/97 16:20 (GMT)	000–190	1–12	540 in-lbs (100% max)
Condition #2	11/21/97 16:20 (GMT)–11/25/97 13:25 (GMT)	195–387	13–148	1080 in-lbs (200% max)

Table 4
Time specification of workload change in TR#12.

	Time period	Time stamp	File number	Workload
Condition #1	2/19/98 21:00 (GMT)–2/23/98 21:00 (GMT)	000–191	1–124	555 in-lbs (100% max)
Condition #2	2/23/98 21:00 (GMT)–2/24/98 07:46 (GMT)	192–222	125–155	1665 in-lbs (300% max)

Table 5
Gearbox information of TR#5 and TR#10.

Gearbox ID#	DS3S0150XX
Make	Dodge APG
Model	R86001
Gear ratio	1.533
Contact ratio	2.388
Number of teeth (driven gear)	46
Number of teeth (pinion gear)	30
Meshing frequency	875.53 (Hz)

Table 6
Gearbox information of TR#12.

Gearbox ID#	DS3S034012
Make	Dodge APG
Model	R86005
Gear Ratio	3.533
Contact Ratio	2.565
Number of teeth (driven gear)	70
Number of teeth (pinion gear)	21
Meshing frequency	613 (Hz)

specification of the gearbox (TR#5 and TR#10) is given in Table 5 and that of the gearbox in TR#12 is given in Table 6.

In TR#5, two adjacent teeth broken of the driven gear were found after test rig shutdown. The total number of running hours is 127.4 h, including 83 data files. In order to keep constant workload, we choose data files with number from 13 to 83, which correspond to vibration data collected under Condition #2. TR#10 was shut down with a distributed gear teeth broken of the driven gear at the end of the test. The total number of running hours is 189.25 h, including 148 data files. Similarly, we choose data files with number from 13 to 148. TR#12 was shut down due to two teeth broken on output gear at the end of the test. The total number of running hours is 106.46 h with 155 data files, in which data files with number from 125 to 155 are selected for analysis. Ref. [2] shows the occurrence of incipient failure for TR#5, TR#10 and TR#12 at time stamp 252, 271 and 208, which correspond to file number 73, 40, 141.

4.2. Evaluation of the proposed health index at different decomposition level

To validate the proposed index FSGI at different wavelet decomposition level, data from TR#5 are used to conduct following analysis. In this comparison, it is necessary to select an optimal detail signal firstly. Therefore, Daubichies-9 wavelet is chosen for signal decomposition and the maximum wavelet decomposition level is 4. Fig. 4 shows the results obtained using the method described in Section 3.2. In this experiment, the fault frequency f_r is 19.0333 Hz. SAI of detail signals at different decomposition levels are calculated and shown in Fig. 4.

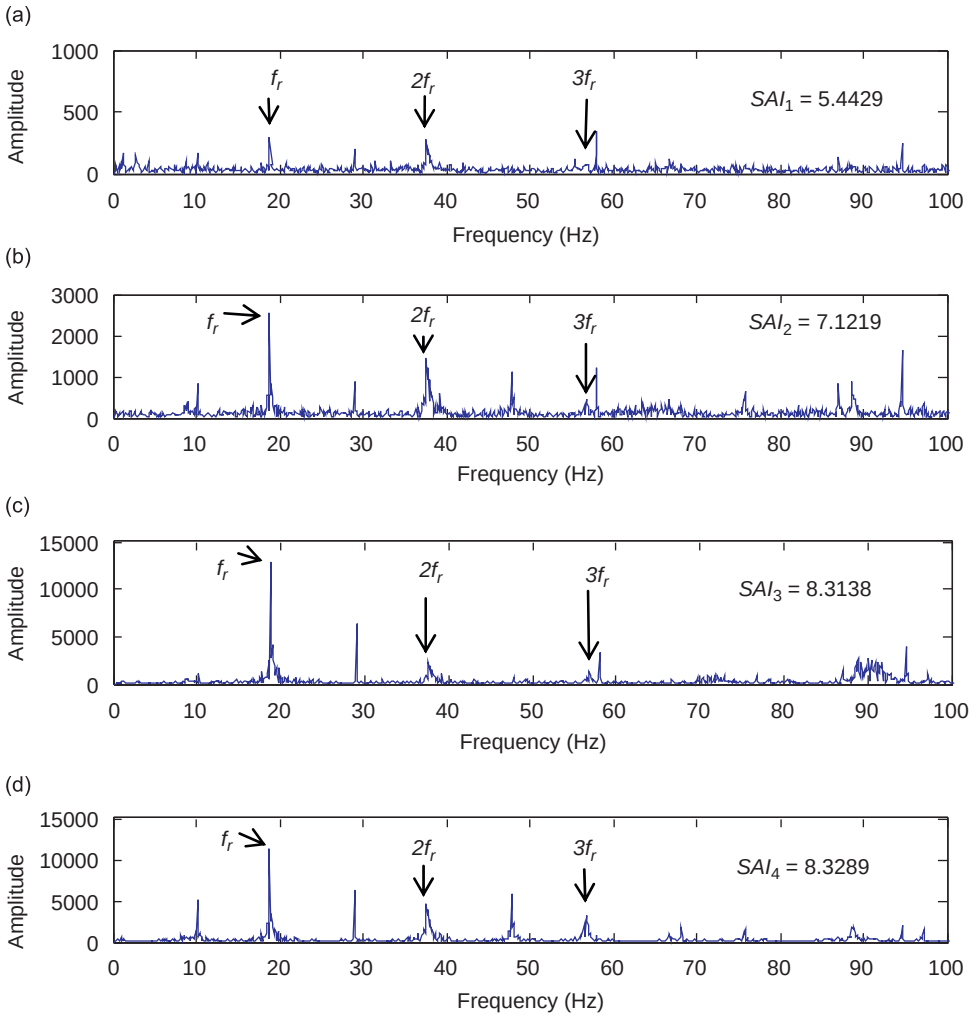

Fig. 4. The results of SAI for selection of detail signal.

According to Eq. (15), the spectrum obtained from $D_4(t)$ should contain lots of useful information to extract gear fault signatures because it has the largest $\mathrm{SAI}_4 = 8.3289$ among all SAI_j. That is to say, the selected optimal signal can precisely reflect fault information on the gear. Therefore, we use $D_4(t)$ for further evaluation of index FSGI in the condition monitoring process.

To evaluate the performance of FSGI at different decomposition levels, we arbitrarily select dB9 and Sym7 wavelets and obtain decomposed detail signals from levels 2 to 7. In this process, the optimal detail signals for decomposition levels 2 and 3 are the second ($D_2(t)$) and the third ones ($D_3(t)$), respectively. For decomposition level at 4, 5, 6 and 7, all the corresponding optimal detail signals are the fourth ones ($D_4(t)$). FSGI index can describe the health condition of gear. Moreover, when FSGI is higher than its corresponding dynamic threshold level for the first time, it means the existence of incipient fault. From the analysis results shown in Figs. 5 and 6, we can see that the proposed health index can identify the occurrence of failure with detail signal at decomposition level of 3, 4, 5, 6 and 7 well. However, for results at decomposition level 2, the proposed FSGI can not identify the occurrence of fault timely due to insufficient decomposition level.

4.3. Evaluation of the proposed health index with different wavelet functions

In order to evaluate the performance of the proposed index FSGI with different wavelets, a comparison is conducted using six wavelet functions including Daubechies wavelet (dB9), Symlet (sym6), Coiflet (coif5),

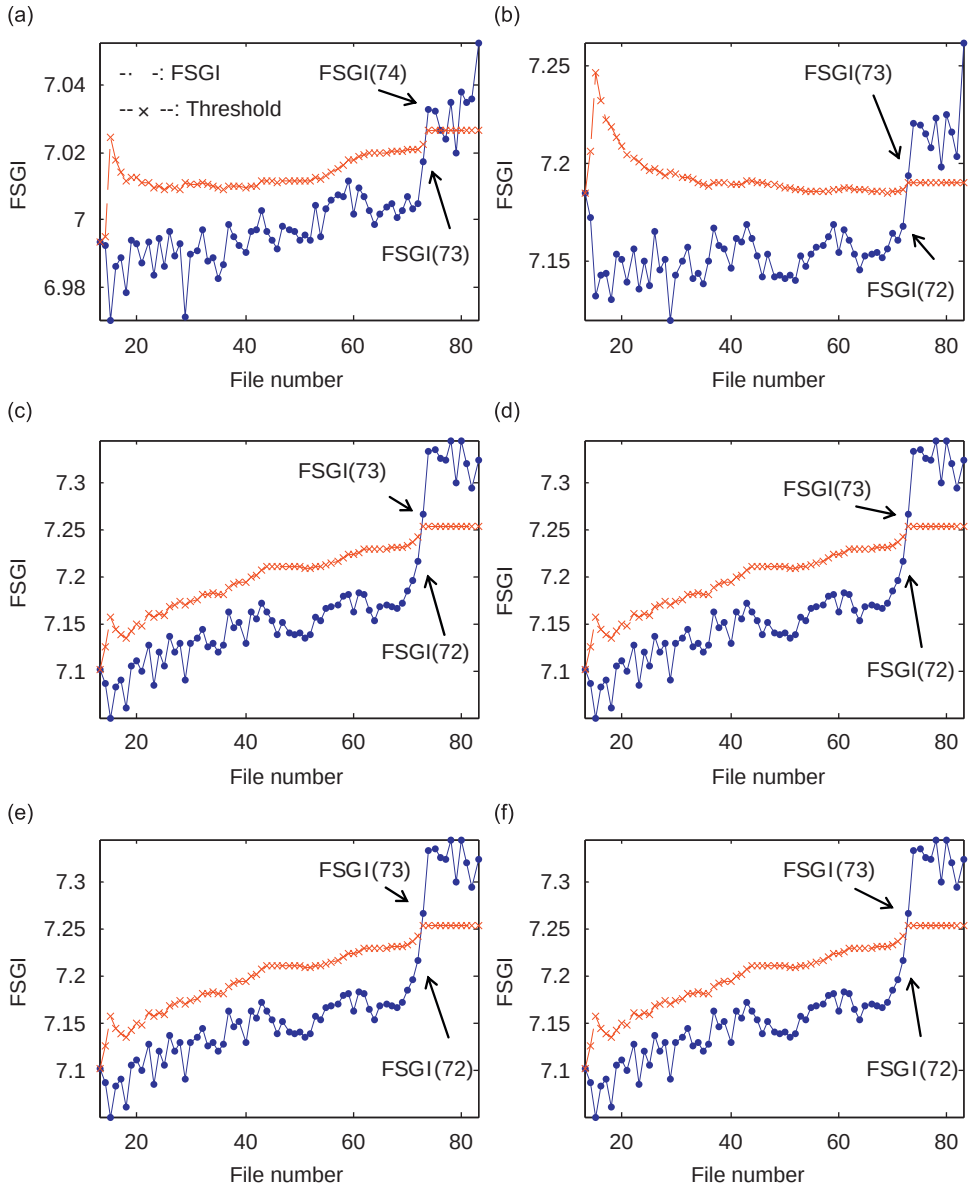

Fig. 5. Comparison results at different wavelet decomposition levels (dB9).

Biorthogonal wavelet (bior4.4), Reverse biorthogonal wavelet (rbio 3.9) and Discrete Meyer wavelet (dmey). According to previous analysis results, we only decompose signal at fourth level and $D_4(t)$ is chosen to calculate the FSGI based on optimal detail signal selection.

The evaluation results with different wavelets are displayed in Fig. 7, which indicate that the proposed method can identify the incipient gear tooth failure with different wavelet functions.

4.4. Evaluation of the proposed health index using Daubechies family with different orders

Daubechies wavelets have following general characteristics: compactly supported wavelets with extremal phase and highest number of vanishing moments for a given support width. Associated scaling filters are minimum-phase filters. If the order of Daubechies wavelet is N, it means parameters of this wavelet such as

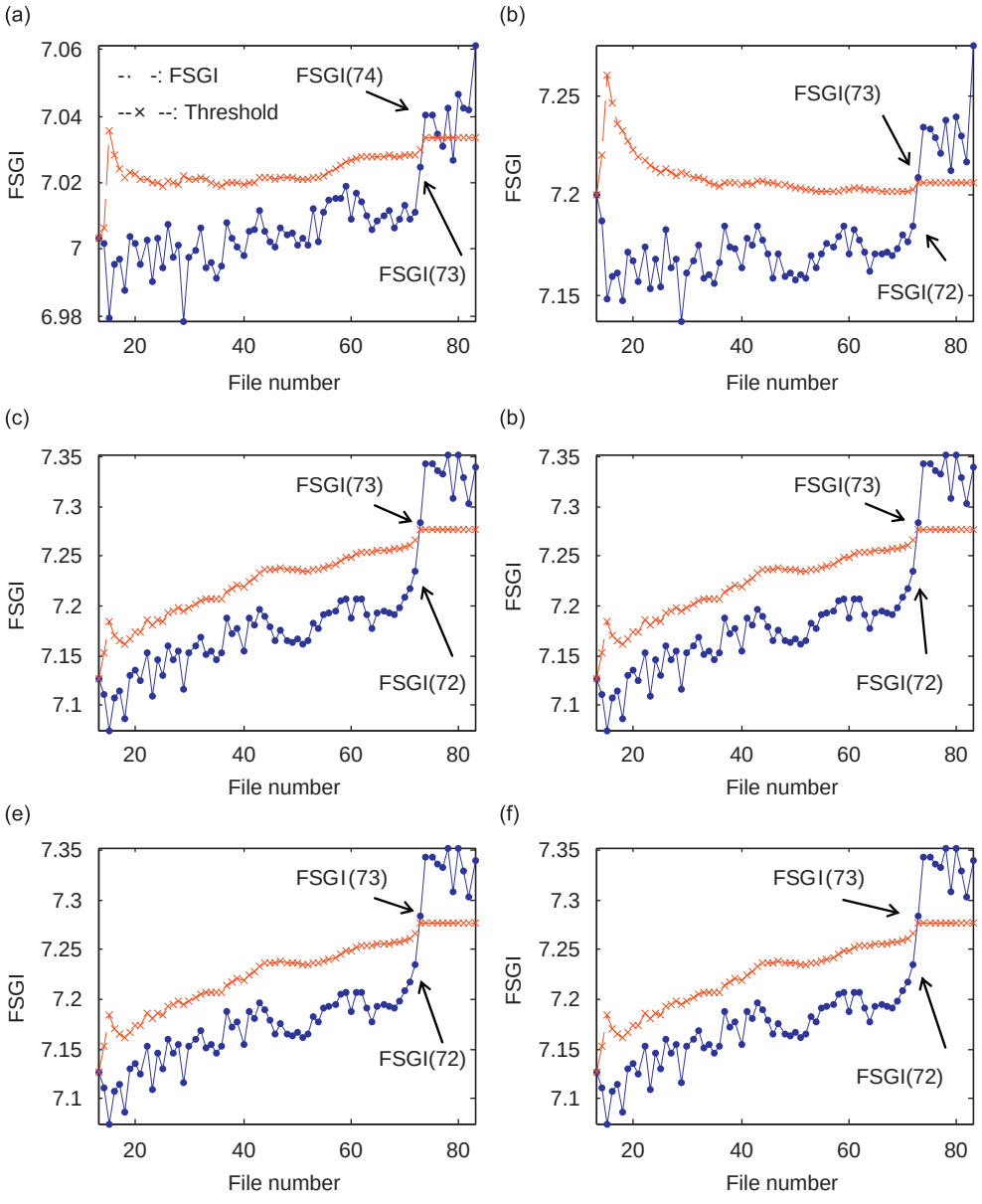

Fig. 6. Comparison results at different wavelet decomposition levels (Sym7).

support width, filters length, regularity and number of vanishing moments are $2N-1$, $2N$, $0.2N$ (for large N) and N, respectively. For fair comparison, we consider the fourth level of decomposition for all Daubechies family wavelet, including dB1 (Haar wavelet), dB3, dB6, dB8, dB10, dB12, dB14 and dB15. The results are shown in Fig. 8 and we can see that the results obtained by different orders are identical, that is to say, the proposed index FSGI is insensitive to the selection of wavelet orders of the same wavelet family.

4.5. Comparison with another method using TR#5, TR#10 and TR#12

In this section, we will compare FSGI with another health index named fault growth parameter 1 (FGP1) [2] using three sets of data (TR#5, TR#10 and TR#12). FGP1 is defined as the part (percentage of points) of the

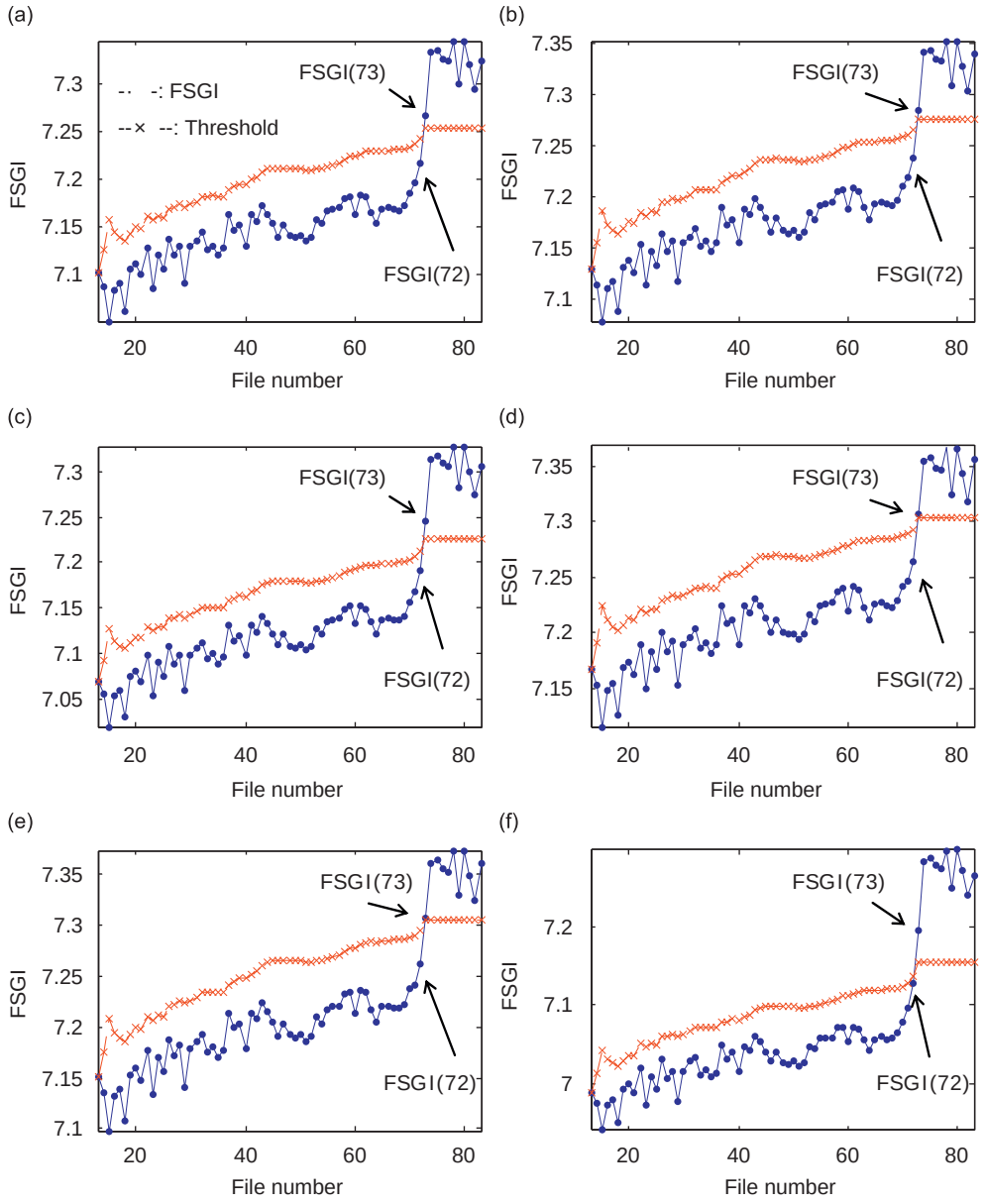

Fig. 7. Comparison results with different wavelets (at the fourth decomposition level).

residual error signal which exceeds three standard deviations calculated from the baseline residual error signal:

$$\mathrm{FGP1} = 100 \sum_{i=1}^{L} \frac{w_i}{W} I(r_i > \overline{r} + 3\sigma_0), \tag{18}$$

where

$$w_i = I(r_i \leqslant \overline{r} + 3\sigma_0) + \left(\left\lfloor \frac{r_i - \overline{r}}{3\sigma_0} - 1 \right\rfloor + 1 \right) I(r_i > \overline{r} + 3\sigma_0), \quad W = \sum_{i=1}^{L} w_i. \tag{19}$$

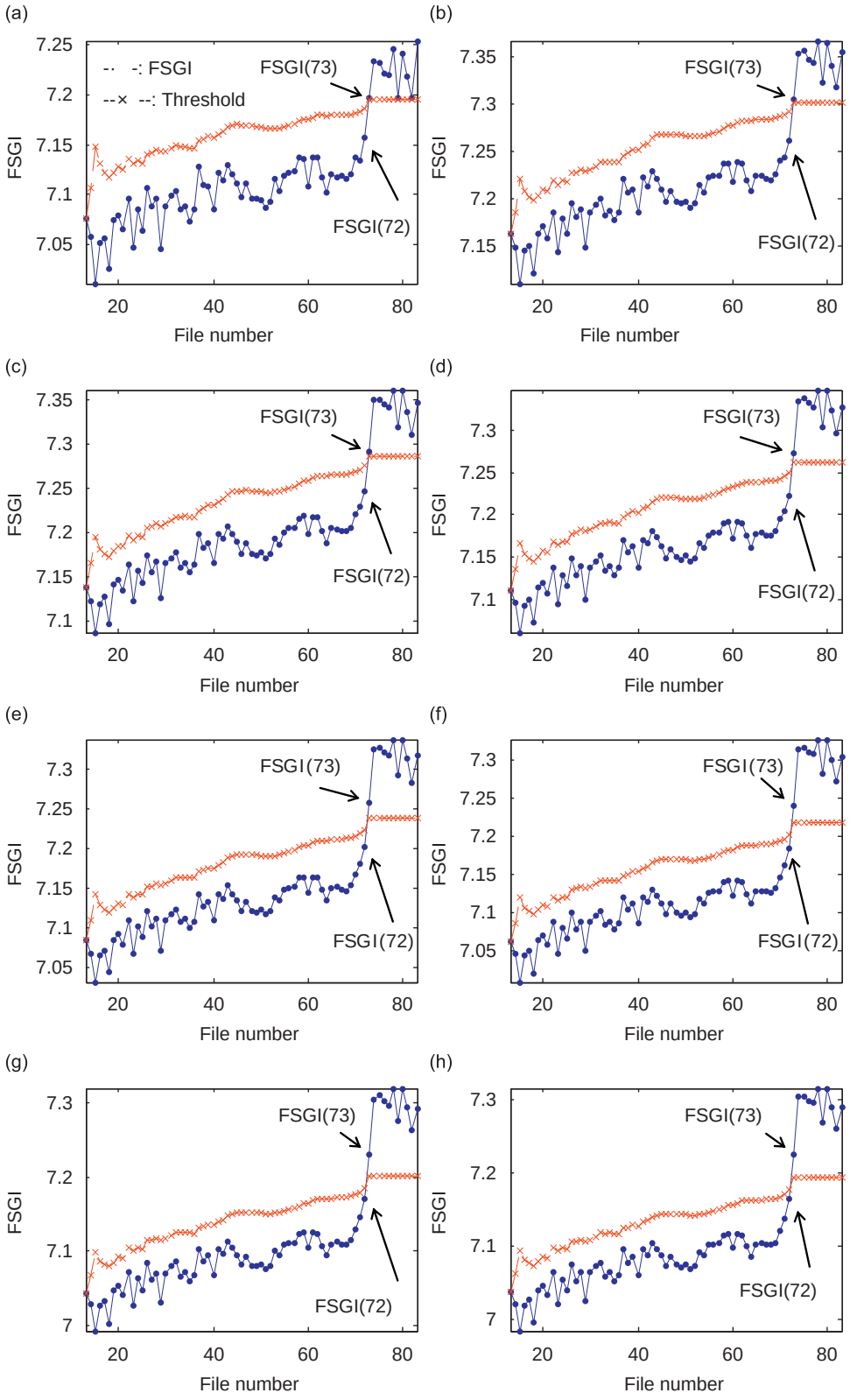

Fig. 8. Comparison results with Daubechies wavelet at different orders.

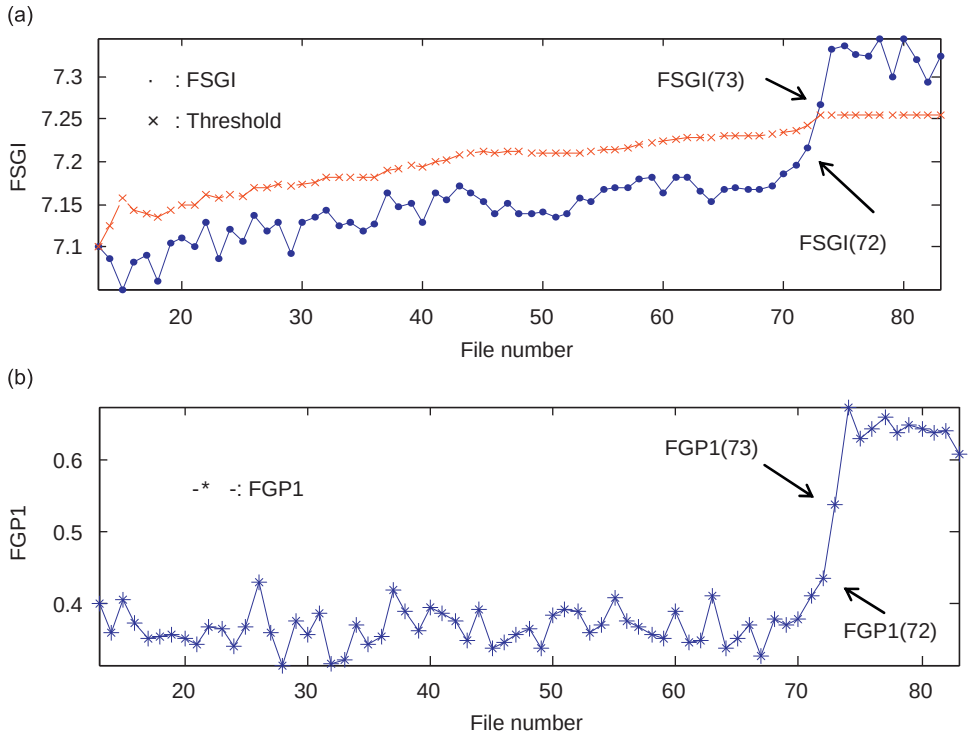

Fig. 9. Comparison results of FSGI and FGP1 using TR#5.

Here r_i's are the current residual error signal points, $\bar{r}$ is the mean value of the current residual signal, σ_0 is the "baseline" standard deviation, $I(\cdot)$ is the indicator function and $\lfloor \cdot \rfloor$ is the floor function. In the computation of FSGI, dB9 wavelet is selected and the optimal detail signal is $D_4(t)$.

Fig. 9 shows the comparison results of FSGI and FGP1 using TR#5. We can find that FSGI increases gradually while the fluctuation of FGP1 is obvious. This means that visual inspection with FSGI is better than FGP1. Another advantage of FSGI is that it owns its corresponding semi-dynamic threshold, which can effectively detect the occurrence of incipient faults. For example, Fig. 9(a) identifies the occurrence of incipient failure at file number 73. Therefore, it is obvious that FSGI is better than FGP1.

In order to comprehensively compare the two indexes, we employ two more sets of data TR#10 and TR#12 to perform condition monitoring. The obtained results are shown in Figs. 10 and 11, respectively. In Fig. 10(b), we can find that the fluctuation of FGP1 is large before the occurrence of early failure. This may result in false alarm in the process of condition monitoring. Fortunately, the performance of FSGI is so great that it can distinguish different conditions between normal and fault in Fig. 10(a). Further, the proposed semi-dynamic threshold can identify the occurrence of early faults at file number 40. In Fig. 11, the development trends of FSGI and FGP1 are much similar. However, FSGI is better than FGP1 because FSGI owns its threshold to automatically detect the change of gear condition.

Furthermore, it should be noted that the computation time is very short with the proposed method. In this research, all the computations are done using MATLAB on an Acer Aspire 4920G laptop with 2.0 GHz CPU and 2 GB RAM. The average times in each experiment (TR#5, TR#10 and TR#12) to compute FSGI and threshold are 0.296, 0.277 and 0.252 s, respectively. Therefore, such a computation speed should be sufficient for on-line condition monitoring.

5. Conclusions

In this paper, we utilize a popular signal processing, wavelet analysis, to decompose vibration. Frequency spectrum growth index (FSGI), together with a semi-dynamic threshold criterion, is proposed in this research

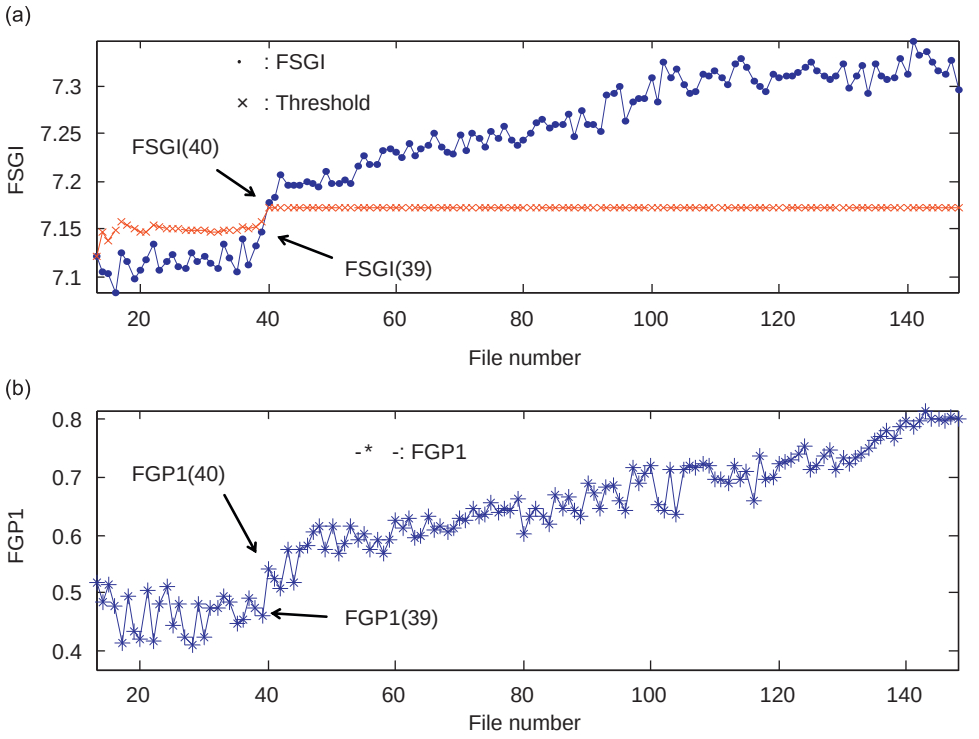

Fig. 10. Comparison results of FSGI and FGP1 using TR#10.

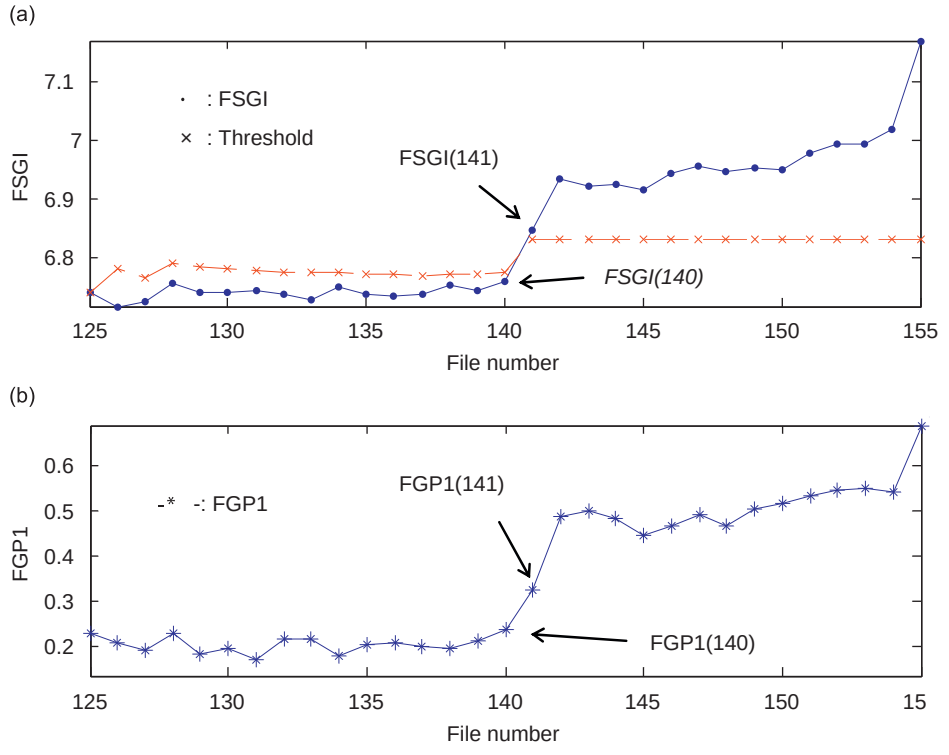

Fig. 11. Comparison results of FSGI and FGP1 using TR#12.

to detect gear faults and describe the health condition of gearbox. Three sets of vibration signals collected from a MDTB is used to validate the proposed method, and analysis results show that FSGI has good performance in gear fault detection. The advantages of this index can be summarized as follows:

(1) It is insensitive to the selection of wavelet function and wavelet decomposition level;
(2) The proposed index FSGI gives a quantitative description of machine health condition, which can be utilized for maintenance decision modeling;
(3) Its computation speed is fast, and it is appropriate for on-line condition monitoring.

Acknowledgments

This research was partially supported by Specialized Research Fund for the Doctoral Program of Higher Education of China (Grant no. 20070614023) and China Postdoctoral Science Foundation Funded Project (Grant no. 20070420223). We are most grateful to the Applied Research Laboratory at the Pennsylvania State University and the Department of the Navy, Office of the Chief of Naval Research (ONR) for providing the vibration data used to develop this work.

References

[1] A.K.S. Jardine, D. Lin, D. Banjevic, A review on machinery diagnostics and prognostics implementing condition-based maintenance, *Mechanical System and Signal Processing* 20 (7) (2006) 1483–1510.
[2] D.M. Lin, M. Wiseman, D. Banjevic, A.K.S. Jardine, An approach to signal processing and condition-based maintenance for gearboxes subject to tooth failure, *Mechanical System and Signal Processing* 18 (5) (2004) 993–1007.
[3] H. Qiu, J. Lee, J. Lin, G. Yu, Wavelet filter-based weak signature detection method and its application on rolling element bearing prognostics, *Journal of Sound and Vibration* 289 (4–5) (2006) 1066–1090.
[4] Z.K. Peng, F.L. Chu, Application of the wavelet transform in machine condition monitoring and fault diagnostics: a review with bibliography, *Mechanical Systems and Signal Processing* 18 (2) (2004) 199–221.
[5] Q. Miao, H.Z. Huang, X.F. Fan, Singularity detection in machinery health monitoring using Lipschitz exponent function, *Journal of Mechanical Science and Technology* 21 (5) (2007) 737–744.
[6] I. Daubechies, Ten Lectures on Wavelets, *CBMS-NSF Series in Applied Mathematics* (*SIAM*), 1991.
[7] S. Mallat, A theory for multiresolution signal decomposition: the wavelet representation, *IEEE Transactions on Pattern Analysis and Machine Intelligence* 11 (7) (1989) 674–693.
[8] P.D. McFadden, Detecting fatigue cracks in gears by amplitude and phase demodulation of the meshing vibration, *ASME Transactions Journal of Vibration Acoustics Stress and Reliability in Design* 108 (1986) 165–170.
[9] X.F. Fan, M. Liang, T.H. Yeap, B. Kind, A joint wavelet lifting and independent component analysis approach to fault detection of rolling element bearings, *Smart Materials and Structures* 16 (5) (2007) 1973–1987.
[10] R. Bussow, An algorithm for the continuous Morlet wavelet transform, *Mechanical Systems and Signal Processing* 21 (8) (2007) 2970–2979.
[11] S. Prabhakar, A.R. Mohanty, A.S. Sekhar, Application of discrete wavelet transform for detection of ball bearing race faults, *Tribology International* 35 (12) (2002) 793–800.
[12] X.F. Fan, M.J. Zuo, Gearbox fault detection using Hilbert and wavelet packet transform, *Mechanical System and Signal Processing* 20 (4) (2006) 966–982.
[13] MDTB Test-run Data CDs, Condition-based Maintenance Department, Applied Research Laboratory, The Pennsylvania State University.